Intermolecular Complexes of HXeOH with Water: Stabilization and Destabilization Effects

ARTICLE *in* JOURNAL OF THE AMERICAN CHEMICAL SOCIETY · OCTOBER 2002

Impact Factor: 12.11 · DOI: 10.1021/ja0266870 · Source: PubMed

6 AUTHORS, INCLUDING:

Markku Rasanen
University of Helsinki
267 PUBLICATIONS **6,962** CITATIONS

SEE PROFILE

J|A|C|S
ARTICLES
Published on Web 08/13/2002

Intermolecular Complexes of HXeOH with Water: Stabilization and Destabilization Effects

Alexander V. Nemukhin,*,† Bella L. Grigorenko,† Leonid Khriachtchev,‡ Hanna Tanskanen,‡ Mika Pettersson,‡ and Markku Räsänen‡

Contribution from the Department of Chemistry, Moscow State University, 119899 Moscow, Russian Federation, and Laboratory of Physical Chemistry, University of Helsinki, P.O. Box 55, FIN-00014 Helsinki, Finland

Received April 26, 2002

Abstract: Theoretical and matrix-isolation studies of intermolecular complexes of HXeOH with water molecules are presented. The structures and possible decomposition routes of the HXeOH$-(H_2O)_n$ ($n =$ 0, 1, 2, 3) complexes are analyzed theoretically. It is concluded that the decay of these metastable species may proceed through the bent transition states (TSs), leading to the global minima on the respective potential energy surfaces, Xe + $(H_2O)_{n+1}$. The respective barrier heights are 39.6, 26.6, 11.2, and 0.4 kcal/mol for $n =$ 0, 1, 2, and 3. HXeOH in larger water clusters is computationally unstable with respect to the bending coordinate, representing the destabilization effect. Another decomposition channel of HXeOH$-(H_2O)_n$, via a linear TS, leads to a direct break of the H−Xe bond of HXeOH. In this case, the attached water molecules stabilize HXeOH by strengthening the H−Xe bond. Due to the stabilization, a large blue shift of the H−Xe stretching mode upon complexation of HXeOH with water molecules is featured in calculations. On the basis of this computational result, the IR absorption bands at 1681 and 1742 cm^{-1} observed after UV photolysis and annealing of multimeric H_2O/Xe matrixes are assigned to the HXeOH$-H_2O$ and HXeOH$-(H_2O)_2$ complexes. These bands are blue-shifted by 103 and 164 cm^{-1} from the known monomeric HXeOH absorption.

1. Introduction

Studies of chemical substances containing rare-gas (Rg) elements continue to attract the attention of research groups, demonstrating a renaissance in this field.[1] A series of species containing rare-gas atoms has been synthesized under various preparative techniques, including low-temperature matrix-isolation methods.[2−5] It is an intriguing question whether molecules of such unusual nature and potentially high reactivity may form stable intermolecular complexes with ordinary molecules. In fact, according to quantum chemistry calculations, HXeH$-(H_2O)_n$ complexes ($n = 1, 2$) should be stable.[6,7] A related and even more important question is whether such molecules may survive in solutions.

Preparation of HRgY molecules (Y is an electronegative fragment) in low-temperature matrixes involves UV photolysis of a HY precursor followed by thermal mobilization of H atoms in the rare-gas lattice.[2] HRgY molecules are formed from neutral H + Rg + Y fragments,[8] their formation consumes a large part of the hydrogen atoms produced during photolysis,[2,9] and the experiments show their intrinsic stability.[10] An important representative of HRgY molecules is HXeOH, formed from H_2O and Xe as described elsewhere.[9,11] It was suggested that HXeOH could be found in aqueous global surroundings, which establishes a high value for studies of HXeOH in water clusters. This consideration is relevant to the known attempts to solve the geochemical "missing Xe" problem,[12] and it might also be connected with understanding the anesthetic properties of Xe.[13]

In this article, we study the complexation of HXeOH with water molecules. It is shown that HXeOH can form stable complexes with water molecules. Like the parent species, HXeOH, the complexes HXeOH$-(H_2O)_n$ are high-energy metastable species that are able to rearrange to thermodynamically more favorable configurations after certain activation. On the basis of the calculated IR absorption spectra, the bands of HXeOH$-(H_2O)_n$ with $n = 1, 2$ in solid Xe are assigned.

* Address correspondence to this author. E-mail: anem@lcc.chem.msu.ru.
† Moscow State University.
‡ University of Helsinki.

(1) Christe, K. O. *Angew. Chem., Int. Ed.* **2001**, *40*, 1419.
(2) Lundell, J.; Khriachtchev, L.; Pettersson, M.; Räsänen, M. *Low Temp. Phys.* **2000**, *26*, 680.
(3) Khriachtchev, L.; Pettersson, M.; Runeberg, N.; Lundell, J.; Räsänen, M. *Nature (London)* **2000**, *406*, 874.
(4) Khriachtchev, L.; Pettersson, M.; Lignell, A.; Räsänen, M. *J. Am. Chem. Soc.* **2001**, *123*, 8610.
(5) Pettersson, M.; Khriachtchev, L.; Lignell, A.; Räsänen, M, Bihary, Z.; Gerber, R. B. *J. Chem. Phys.* **2002**, *116*, 2508.
(6) Lundell, J.; Pettersson, M. *Phys. Chem. Chem. Phys.* **1999**, *1*, 1691.
(7) Lundell, J.; Berski, S.; Latajka, Z. *Phys. Chem. Chem. Phys.* **2000**, *2*, 5521.
(8) Pettersson, M.; Nieminen, J.; Khriachtchev, L.; Räsänen, M. *J. Chem. Phys.* **1997**, *107*, 8423.
(9) Khriachtchev, L.; Tanskanen, H.; Pettersson, M.; Räsänen, M., Ahokas, J.; Kunttu, H.; Feldman, V. *J. Chem. Phys.* **2002**, *116*, 5649.
(10) Lorenz, M.; Räsänen, M.; Bondybey, V. E. *J. Phys. Chem. A* **2000**, *104*, 3770.
(11) Pettersson, M.; Khriachtchev, L.; Lundell, J.; Räsänen, M. *J. Am. Chem. Soc.* **1999**, *121*, 11904.
(12) Caldwell, W. A.; Nguyen, J. H.; Pfrommer, B. G.; Mauri, F.; Louie, S. G.; Jeanloz, R. *Science* **1997**, *277*, 930 and references therein.
(13) LaBella, F. S.; Stein, D.; Queen, G. *Eur. J. Pharmacol.* **1999**, *381*, R1.

10.1021/ja0266870 CCC: $22.00

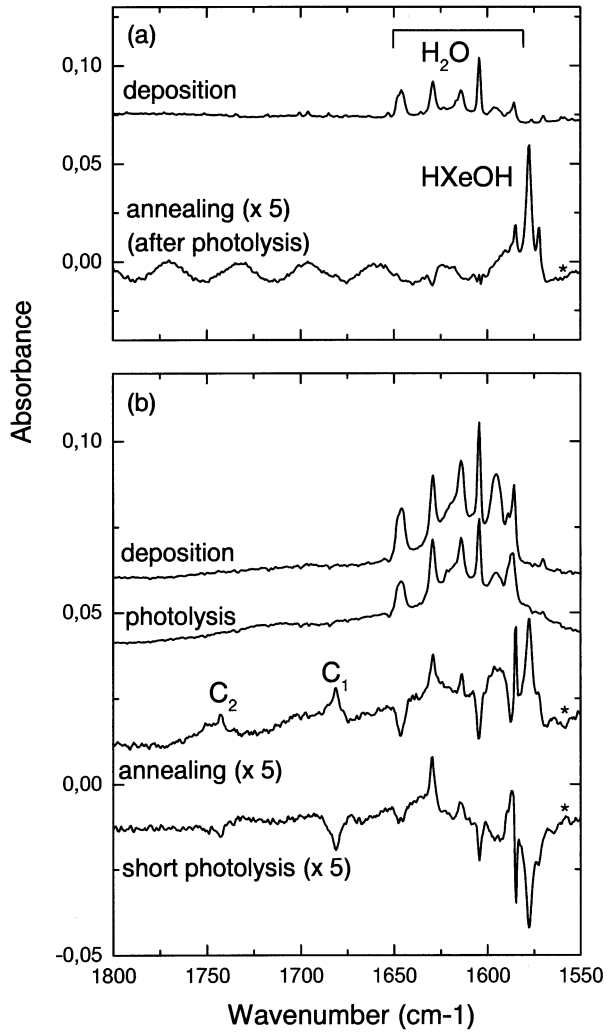

Figure 1. FTIR spectra of H_2O/Xe solid mixtures at various experimental stages (deposition, photolysis, annealing). Sample b is more concentrated than sample a. The spectra marked with asterisks refer to the difference spectra obtained as a result of annealing and short photolysis. Peaks marked with C_1 and C_2 in plot b are assigned to the HXeOH−(H_2O) and HXeOH−(H_2O)$_2$ complexes, respectively. Some changes in the monomer water bands upon annealing and short photolysis are explained by slow redistribution between the rotational sublevels.

2. Experimental Section

The Xe matrixes containing water molecules were prepared by using co-deposition of Xe gas and water vapor from two separate nozzles controlling the relative flux with calibrated needle valves.[9] The H_2O/Xe matrixes were deposited on a CsI substrate kept at 30 K, the deposition time was ∼1 h, and the typical matrix thickness was 100 μm. IR absorption measurements were performed at 7 K in a closed-cycle helium cryostat (APD, DE-202A). IR absorption spectra in the 4000−400 cm^{-1} region were recorded with a Nicolet 60 SX FTIR spectrometer using resolution of 1 cm^{-1} and co-adding 500 scans. To decompose water, the samples were irradiated with an excimer laser (MPB, MSX-250) operating at 193 nm, typically using $\sim 2 \times 10^3$ pulses with pulse energy density of ∼10 mJ/cm^2.

The IR absorption spectrum of water in solid Xe in the H_2O bending region is presented in Figure 1 by the upper traces, the H_2O concentration being higher in plot b. The strongest IR absorption bands of monomeric H_2O in this region are at 1605, 1614, 1629, and 1646 cm^{-1}, and the band of (H_2O)$_2$ is at 1586 cm^{-1}.[9] The 1595 cm^{-1} band belongs to (H_2O)$_3$ and higher multimers. A band of nonrotating water is probably close to that of the water dimer, analogous to the data in Kr and Ar matrixes.[14]

Upon irradiation at 193 nm, water decomposes and the IR absorption band for OH radicals appears, as evidenced by laser-induced fluorescence and the IR absorption band at 3531.2 cm^{-1}.[15] Annealing of the photolyzed samples with water monomers at 45 K efficiently mobilizes H atoms, and HXeH (1166.4 and 1180.1 cm^{-1}) and HXeOH (1577.6 cm^{-1}) are formed (see Figure 1a for HXeOH).[2,11]

Upon photolysis of samples with water multimers, the decomposition of the multimers is quite efficient, but the decomposition of the monomers is rather limited. The photolysis efficiency is diminished for the present case of concentrated water matrixes due to strongly rising absorption by caged H atoms (self-limitation of photolysis[16]). On the other hand, the decomposition of the water multimers might be enhanced due to a complexation-induced shift of the absorption in the UV spectral region. As a result of the decomposition of water dimers, the buildup of the band at 3403 cm^{-1} of the OH−H_2O complex is remarkable.[9,17] Upon annealing at 45 K of multimeric samples, two additional bands at 1681 and 1742 cm^{-1} rise (see Figure 1b) that are absent in the monomeric sample. From the experimental evidence, it is plausible to assign these bands to the H−Xe stretches of HXeOH−H_2O (C_1) and HXeOH−(H_2O)$_2$ (C_2), respectively, or to two different configurations of HXeOH−H_2O. Upon annealing, the 3403 cm^{-1} band decreases, which indicates that the reaction of the OH−H_2O complex with mobile H atoms produces the HXeOH−H_2O complex.

The Xe-containing molecules are known to be unstable under UV irradiation, providing a sensitive test.[9,11] Upon very short (∼50 pulses) irradiation at 193 nm, the three bands at 1578, 1681, and 1742 cm^{-1} synchronously bleached, as shown by the lower trace of Figure 1b, and this supports the participation of the Xe-containing molecules in bands at 1681 and 1742 cm^{-1}. Upon such short photolysis, the OH−H_2O band quantitatively recovers, supporting participation of this fragment in the destroyed species.

3. Quantum Chemistry Modeling

Structures and IR Spectra of HXeOH−(H_2O)$_n$. Quantum chemistry calculations have been carried out with the GAMESS package[18] or, more specifically, with its version for Intel-based workstations, PC GAMESS.[19] In all calculations, we used the aug-cc-pVTZ basis sets for oxygen and hydrogen with additional diffuse s-functions for hydrogen, since we expect formation of the fragment XeH with a slight negative charge on H.[11] The energy-adjusted pseudopotential of Nicklass et al.[20] (the non-relativistic version) and the corresponding (6s6p1d)/[4s4p1d] basis functions for Xe are employed. With these options, the MP2 calculations result in the value 12.2 eV for the ionization potential of Xe, which coincides exactly with the reference data of Nicklass et al.[20] (the experimental estimate cited in ref 20 is 12.6 eV). The computed molecular constants of diatomic species XeH^+ (R_e = 1.605 Å, ω_e = 2324 cm^{-1}) are similar to those published previously by Lundell et al.[21] (R_e = 1.58 Å, ω_e = 2423 or 2388 cm^{-1}) and to the experimental estimates cited in ref 21 (R_e = 1.603 Å, ω_e = 2270 cm^{-1}). At the MP2 level, the electron affinity of OH is computed as 1.94 eV, while the

(14) Engdahl A.; Nelander, B. *J. Mol. Struct.* **1989**, *193*, 101.
(15) Pehkonen, S.; Pettersson, M.; Lundell, J.; Khriachtchev, L.; Räsänen, M. *J. Phys. Chem. A* **1998**, *102*, 7643.
(16) Khriachtchev, L.; Pettersson, M.; Räsänen, M. *Chem. Phys. Lett.* **1998**, *288*, 727.
(17) Khriachtchev, L.; Pettersson, M.; Jolkkonen, S.; Pehkonen, S.; Räsänen, M. *J. Chem. Phys.* **2000**, *112*, 2187.
(18) Schmidt, M. W.; Baldridge, K. K.; Boatz, J. A.; Elbert, S. T.; Gordon, M. S.; Jensen, J. H.; Koseki, S.; Matsunaga, N.; Nguyen, K. A.; Su, S. J.; Windus, T. L.; Dupuis, M.; Montgomery, J. A. *J. Comput. Chem.* **1993**, *14*, 1347.
(19) Granovsky, A. A. URL: http:/lcc.chem.msu.ru/gran/gamess/index.html
(20) Nicklass, A.; Dolg, M.; Stoll, H.; Preuss, H. *J. Chem. Phys.* **1995**, *102*, 8942.
(21) Lundell, J.; Nieminen, J.; Kunttu, H. *Chem. Phys. Lett.* **1993**, *208*, 247.

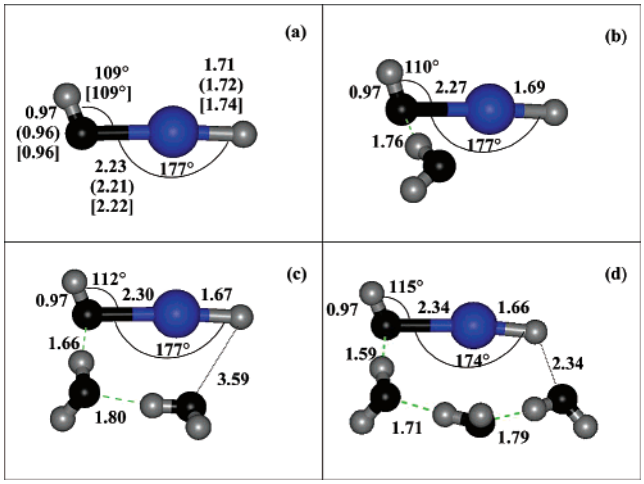

Figure 2. Equilibrium geometry configurations of the main isomers of the HXeOH−$(H_2O)_n$ complexes (n = 0, 1, 2, 3) according to the present MP2 calculations. Distances are given in angstroms. Panel a shows the results for n = 0 of the previous[11] calculations: MP2 in parentheses and CCSD(T) in square brackets.

Table 1. Computed Harmonic Frequencies and Relative IR Intensities (in Parentheses) of HXeOH (cm^{-1})

mode	MP2, ref 11	CCSD(T), ref 11	MP2, this work
O−H stretch	3842 (0.04)	3836	3744 (0.04)
Xe−H stretch	1823 (1.00)	1678	1790 (1.00)
H−Xe−O−H antisymmetric bend	819 (0.00)	812	832 (0.00)
H−Xe−O bend	652 (0.00)	630	647 (0.00)
H−Xe−O−H symmetric bend	584 (0.01)	574	595 (0.01)
Xe−OH stretch	436 (0.09)	419	441 (0.13)

experimental value is 1.83 eV.[22] It has been shown previously[23] that calculations with the aug-cc-pVTZ basis sets allowed one to describe correctly potential energy curves of ion-pair states of OH, as well as the anion OH^-. Therefore, we consider this level of treatment adequate for the goals of the present study.

The basic unit, namely, the HXeOH species, was characterized previously by quantum chemistry calculations at the MP2 and CCSD(T) levels with the effective core potential LJ18 and the corresponding valence basis set for Xe and the standard 6-311++G(2d,2p) sets for O and H. [11] As illustrated in Figure 2a, our approach gives essentially the same equilibrium geometry for the almost planar molecule HXeOH. The electronic structure of HXeOH may be described in terms of the natural bond orbital (NBO) analysis.[24] According to this methodology, two bonding orbitals, σ(OH) and σ(XeH), are consistent with the electronic distribution in the system. The computed natural charges on atoms, $H^{-0.084}Xe^{+0.839}O^{-1.212}H^{+0.457}$, indicate a highly ionic contribution to the binding.

Table 1 compares the harmonic frequencies and relative IR intensities of HXeOH computed in this work and in ref 11. The experimentally observed band of the Xe−H stretching vibration is at 1578 cm^{-1}. According to all calculations, this is the most intense IR band in the vibrational spectrum. The difference between the observed frequency and theoretical estimates at the MP2 and CCSD(T) levels (100−200 cm^{-1}) can be attributed to matrix effects and anharmonic contributions.

The equilibrium configurations for the HXeOH−$(H_2O)_n$ species (n = 0, 1, 2, 3) obtained by the present MP2 calculations are shown in Figure 2. The arrangement of water molecules around HXeOH is reasonable: they form a hydrogen-bonded network including the OH fragment of the HXeOH molecule, whose properties resemble closely the properties of the hydroxyl anion OH^-. However, some influence of the positively charged Xe atom interacting with the water oxygens is noticeable, and instead of further hydrating the hydroxyl group, water molecules form chains spread along the O−Xe−H axis, as shown in Figure 2. According to the NBO analysis, the surrounding water molecules bear slight negative charges between −0.01 and −0.05.

Analysis of the equilibrium structures HXeOH−$(H_2O)_n$ leads to the conclusion that surrounding water molecules can stabilize the HXeOH monomer by strengthening the Xe−H bond. The computed properties collected in Figure 2 and in Table 2 illustrate this trend. When the number of attached water molecules increases, the Xe−H bond length shortens, the partial charge on the XeH fragment increases, the energy assigned by the NBO analysis to the XeH orbital decreases, and the frequency of the Xe−H stretching vibration increases.

Alternative arrangements of water molecules have been also considered, but for n = 1 no more isomers have been found. For n = 2 and n = 3, the new structures of HXeOH−$(H_2O)_2$ and HXeOH−$(H_2O)_3$, in which the water molecules are grouped around the OH-fragment, correspond to true local minima on the respective potential energy surfaces with energies, which are 0.7 and 3.7 kcal/mol higher than those of the main isomers, shown in Figure 2c,d. The Xe−H stretching frequencies in these higher energy isomers are 2012 cm^{-1} for n = 2 and 2088 cm^{-1} for n = 3, and they are further blue-shifted compared to the frequencies of the lowest energy structures (1972 cm^{-1} for n = 2 and 2066 cm^{-1} for n = 3). Taking into account the very small energy differences between the isomers, we cannot exclude that all these higher energy species are formed in the experiments. However, in the following discussions we focus on the lowest energy configurations, and unless additionally specified, the symbols HXeOH−$(H_2O)_n$ will refer to the main isomers illustrated in Figure 2.

The configurations shown in Figure 2 correspond to highly energetic local minima on the entire potential energy surfaces of the HXeOH−$(H_2O)_n$ systems. The global minima refer to the complexes of xenon with water clusters Xe−$(H_2O)_{n+1}$, the energies of which are about 100 kcal/mol lower. In the last row of Table 2, we collect the computed energies of HXeOH−$(H_2O)_n$ with respect to the points Xe + (n + 1)H_2O (n = 0, 1, 2, 3). If we combine these values with the estimates for the binding energies of water clusters $(H_2O)_{n+1}$ (e.g., ref 25) as 5.4 (n = 1), 15.9 (n = 2), and 27.6 kcal/mol (n = 3), then the energy differences between the systems HXeOH−$(H_2O)_n$ and Xe−$(H_2O)_{n+1}$ are almost constant (109.5, 104.1, 103.6, 104.0 kcal/mol for n = 0, 1, 2, 3, respectively). Interaction of the xenon atom with water molecules will add some extra binding energy, but these amounts should not be large. It should be noted that no BSSE corrections have been taken into account in these energy estimates.

(22) Schulz, P. A.; Mead, R. A.; Jones, P. L.; Lineberger, W. C. *J. Chem. Phys.* **1982**, *77*, 1153.
(23) Nemukhin, A. V.; Grigorenko, B. L. *Chem. Phys. Lett.* **1997**, *276*, 171.
(24) Reed, A. E.; Curtiss, L. A.; Weinhold, F. *Chem. Rev.* **1988**, *88*, 899.
(25) Grigorenko, B. L.; Nemukhin, A. V.; Topol, I. A.; Burt, S. K. *J. Chem. Phys.* **2000**, *113*, 2638.

Table 2. Computed Properties of the Complexes HXeOH−$(H_2O)_n$

property	$n = 0$	$n = 1$	$n = 2$	$n = 3$
distributions of natural charges	$(OH)^{-0.76}(XeH)^{+0.76}$	$(OH)^{-0.77}(XeH)^{+0.80}$	$(OH)^{-0.78}(XeH)^{+0.83}$	$(OH)^{-0.80}(XeH)^{+0.86}$
orbital energies ϵ(XeH), au	−0.649	−0.675	−0.682	−0.687
Xe−H stretch frequencies, cm^{-1}, and relative IR intensities	1790 (1.00)	1897 (0.77)	1972 (0.58)	2066 (0.15)
energy (kcal/mol) with respect to Xe + $(n + 1)H_2O$	109.5	98.7	87.7	76.4

Table 3. Properties of the Transition-State (TS) Structures Shown in Figure 3 (MP2 Results)

property	$n = 0$	$n = 1$	$n = 2$	$n = 3$
energy barrier with respect to HXeOH−$(H_2O)_n$, kcal/mol	39.6	26.6	11.2	0.4
imaginary frequency of TS, cm^{-1}	476i	572i	679i	171i
natural charges on atoms	$H^{+0.45}O^{-1.43}Xe^{+0.80}H^{+0.18}$	$H^{+0.46}O^{-1.36}Xe^{+0.78}H^{+0.22}$	$H^{+0.47}O^{-1.34}Xe^{+0.71}H^{+0.21}$	$H^{+0.46}O^{-1.29}Xe^{+0.74}H^{+0.13}$
orbital energy ϵ(XeH), au	−0.798	−0.789	−0.725	−0.693

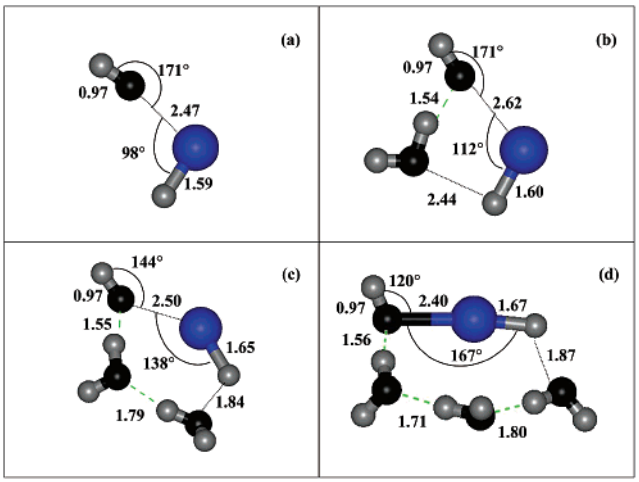

Figure 3. Geometry configurations of the bent transition states for decomposition of the HXeOH−$(H_2O)_n$ complexes ($n = 0, 1, 2, 3$) to the products Xe−$(n + 1)H_2O$ according to the present MP2 calculations. Distances are given in angstroms.

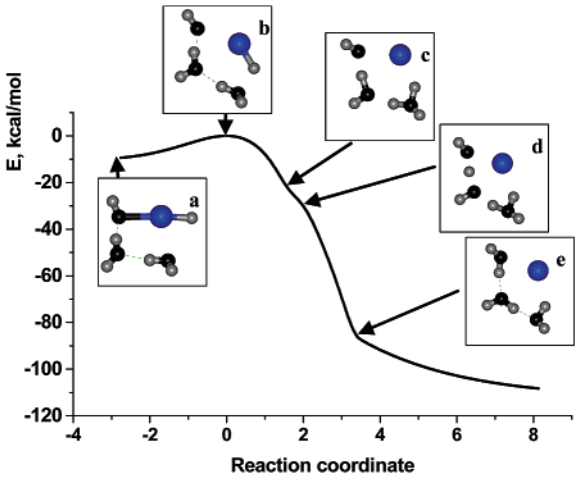

Figure 4. Reaction path specified by the intrinsic reaction coordinate MP2 calculations in both directions from the transition state for the decomposition HXeOH−$(H_2O)_2$ → Xe−$(H_2O)_3$.

If we compare the computed harmonic frequencies and IR intensities of the HXeOH−$(H_2O)_n$ ($n = 0, 1, 2$) complexes with the corresponding peaks in the experimental spectrum of Figure 1, we notice a remarkable similarity between theoretical and experimental results. This similarity becomes more visible if we apply the scaling factor (0.88) for the computed frequencies, which gives precise coincidence between the computed (1790 cm^{-1}) and experimental (1578 cm^{-1}) H−Xe stretching frequencies of the HXeOH monomer. After this manipulation, the scaled theoretical spectral lines for HXeOH−(H_2O) and HXeOH−$(H_2O)_2$ (1669 and 1735 cm^{-1}) may be directly assigned to the experimental peaks (1681 and 1742 cm^{-1}).

Decomposition Routes of HXeOH−$(H_2O)_n$. The metastable species shown in Figure 2 can survive if the potential barriers separating these local minima from the lower energy regions of the energy surfaces are high enough. First, we study decomposition routes of the complexes HXeOH−$(H_2O)_n$ leading to the global minima Xe + $(n + 1)H_2O$ on the corresponding potential energy surfaces. Figure 3 shows the geometry of the transition states (TSs) found at the MP2 level, and Table 3 collects selected parameters for these TSs.

Analyzing these data, we notice that the decomposition of HXeOH−$(H_2O)_n$ toward global minima proceeds through the bent TSs, which keep some features of $(OH)^-(XeH)^+$ complexed with water molecules. Compared to the equilibrium geometry shown in Figure 2, the Xe−O distances increase in the bent TSs for all n, but the Xe−H distances decrease. According to the NBO analysis, the energies attributed to the XeH bonding orbitals are even lower in transition states than those in the equilibrium configurations (see Table 2). The changes in the geometry, when passing from the equilibrium to the TS structures (compare Figures 2 and 3), decrease with n, and the TS geometry is very close to that of HXeOH−$(H_2O)_3$. On the basis of this analysis, the species HXeOH (barrier 39.6 kcal/mol), HXeOH−(H_2O) (barrier 26.6 kcal/mol), and HXeOH−$(H_2O)_2$ (barrier 11.2 kcal/mol) should be stable with respect to the bending reaction coordinate. The complex with three water molecules (barrier 0.4 kcal/mol) is hardly stable in this respect. The tendency for barrier heights in these bent TSs is consistent with the decreasing frequencies of the corresponding bending vibration in the equilibrium configurations of the complexes HXeOH−$(H_2O)_n$ (832, 788, 770, and 714 cm^{-1} for $n = 0, 1, 2,$ and 3, respectively).

Calculation of the steepest-descent pathways along the intrinsic reaction coordinate, starting from the saddle points in both directions, confirmed the assignment of these transition states to the energy paths connecting the systems HXeOH−$(H_2O)_n$ and Xe−$(H_2O)_{n+1}$. In Figure 4, we show this reaction pathway for $n = 2$. The equilibrium configuration of the HXeOH−$(H_2O)_2$ complex (the inner well) and the configuration of TS (the top) are shown in panels a and b. Upon progressing to the reaction product (to the right in the graph), the system undergoes transformations, which can be described as a proton

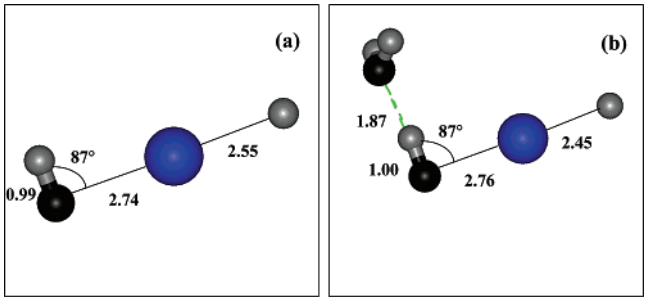

Figure 5. Geometry configurations of the linear transition states for decomposition of the HXeOH−$(H_2O)_n$ complexes ($n = 0$, 1) by the direct break of the Xe−H bond. The results are those of the present MP2 calculations. Distances are given in angstroms.

transfer along a water wire. After leaving the bent TS, the Xe−H bond breaks, and the released proton jumps to the nearest water molecule (panel c). According to NBO analysis at this point of the reaction path, the system can be viewed as the ion pair $(OH)^{-0.85}$ and $(H_3O)^{+0.72}$, separated by a water molecule $(H_2O)^{-0.08}$, and bound to the Xe atom with a partial charge +0.20. The next step in the transformation corresponds to the structure shown in panel d. Here, NBO analysis suggests the ion pair $(OH\cdots H\cdots OH)^{-0.87}$ and $(H_3O)^{+0.74}$, bound to the Xe atom with a partial charge +0.13. The last section of the energy curve refers to the final stage of the proton-transfer process (panel e), where the xenon atom is bound to the three water molecules.

An alternative channel to decompose HXeOH and its complexes with water is a direct break of the Xe−H bond. In our MP2 calculations, the energy of the Xe + H + OH asymptote is 13.5 kcal/mol higher with respect to the energy of HXeOH, in agreement with another computed value of 13.8 kcal/mol.[11] We found the corresponding TSs at the MP2 level for the cases of $n = 0$ and $n = 1$ (see Figure 5). For $n = 2$ and $n = 3$, all suggested configurations for linear transition states finally evolved to the known bent TSs.

These TS structures correspond to an almost linear arrangement of the O−Xe−H fragment. The imaginary frequencies are 797i for $n = 0$ and 700i for $n = 1$. For $n = 0$, the computed energy barrier with respect to the local minimum HXeOH (28.2 kcal/mol) is lower than the activation energy through the bent transition state (39.6 kcal/mol). For $n = 1$, the activation barrier through the linear TS (34.1 kcal/mol) is higher than that of the bent TS (26.6 kcal/mol). Again we notice that the attached water molecule strengthens the Xe−H bond (34.1 kcal/mol for $n = 1$ vs 28.2 kcal/mol for $n = 0$), demonstrating the stabilization effect.

There might be some doubts about whether the MP2 wave functions correctly describe the decomposition route HXeOH → H + Xe + OH. To check the above conclusions, we carried out the calculations using the multiconfigurational CASSCF wave functions with an additional treatment of electron correlation at the multiconfigurational quasi-degenerate perturbation theory (MCQDPT).[26] The CASSCF functions included 45 configurations with the oxygen 1s orbital always doubly occupied and nine MOs populated by 16 valence electrons. This scheme is consistent with partial occupation of the Xe−H bonding and antibonding orbitals. The equilibrium configurations of HXeOH at the CASSCF and MCQDPT levels were in reasonable accord with the MP2 and CCSD(T) results. In fact, the O−H(O-bound), O−Xe, and Xe−H(Xe-bound) distances were 0.95, 2.23, and 1.78 Å (CASSCF) and 0.97, 2.22, and 1.79 Å (MCQDPT), respectively. The linear TS structure with a single imaginary frequency of 553i at the CASSCF level corresponded to the species with an almost linear arrangement O−Xe−H and O−Xe and Xe−H distances of 2.37 and 1.96 Å, respectively. The CASSCF energy barrier for decomposition was obtained as only 1.04 kcal/mol. Obviously, the lack of electron correlation, especially for the Xe−O interactions, prevented reasonable calculations of the energies with such a CASSCF wave function. At the MCQDPT level, we could not compute the frequencies; therefore, only estimates were performed for the barrier height. We found that the saddle point was located at a Xe−H distance of about 2.40 Å, and the energy barrier was close to 15.2 kcal/mol. From this series of calculations, it seems that the route for decomposition of HXeOH through direct breaking of the Xe−H bond should proceed through the barrier, and the barrier height for HXeOH might be lower than that of the channel through the bent TS (39.6 kcal/mol according to the MP2 calculations).

It should be emphasized that the present theory is applied to isolated HXeOH−$(H_2O)_n$ species, and the experimental conditions of matrix isolation may essentially change the conclusions about the stability of these complexes. The known cage effect may stabilize complexes with three or more water molecules in the matrix. In the experimental conditions, detection of complexes with one and three water molecules seems to be justified, but formation of higher associates ($n \geq 3$) is still questionable. Chances for stabilization of HXeOH−water complexes are related to the occurrence of structures with a diminished role of decomposition through proton transfer from $(XeH)^+$ to water. The role of lattice rare-gas atoms may be important in this respect. The matrix effects refer not only to the matrix-induced shifts of spectral bands and the cage effects, but also to other stabilization and destabilization effects of interactions with the matrix material. It is known that the ionic species XeH^+ does not survive in xenon matrixes, and instead, the three-atom anions $XeHXe^+$ are formed.[27,28] Ab initio calculations at the MP2 level show that the HXeOH−Xe system corresponds to a local minimum on the potential energy surface, with the additional xenon atom far from the HXeOH molecule (the Xe−Xe distance is almost 5 Å). Initial calculations for the decomposition of HXeOH−Xe to $OH^- + XeHXe^+$ resulted in a gradual increase of energy with no barriers on the reaction route. To formulate more definite conclusions about the structure and stability of the complexes HXeOH−$(H_2O)_n$ in solid xenon, obviously, a special treatment is required.

The Case of Large *n*. We also considered the HXeOH−$(H_2O)_n$ structures with a larger number of water molecules (up to 30) and tried to construct cages of water molecules around the basic HXeOH unit and to estimate the influence of these cages on the decomposition potential energy profiles of HXeOH. The quantum mechanical−molecular mechanical (QM/MM) approach of effective fragment potentials[29] was applied to describe interactions of several water molecules with the central

(26) Nakano, H. *J. Chem. Phys.* **1993**, *99*, 7983.
(27) Kunttu, H.; Seetula, J.; Räsänen M.; Apkarian, V. A. *J. Chem. Phys.* **1992**, *96*, 5630.
(28) Beyer, M. K. Ph.D. Dissertation, Technical University of Munich, 1999.
(29) Gordon, M. S.; Freitag, M. A.; Bandyopadhyay, P.; Jensen, J. H.; Kairys, V.; Stevens, W. J. *J. Phys. Chem. A* **2001**, *105*, 293.

unit HXeOH. At this level of theory, multiple sets of configurations $HXeOH-(H_2O)_n$ ($n \leq 30$) were constructed as the corresponding points of local minima on the corresponding potential surfaces. All configurations that allowed the "tail" Xe−H of HXeOH to stay relatively far from water molecules corresponded to true minima, and the effect of water molecules strengthening the Xe−H bond noticed for a few ($n = 1, 2, 3$) species was confirmed. This network was completely ruined when the effective fragments for water molecules were replaced by the quantum systems, and practically all found structures collapsed. The reasons for that are finally clear: despite some stabilization of the Xe−H bond, the surrounding water molecules enhance decomposition of HXeOH through the bent transition states, i.e., the destabilization factor is stronger.

4. Conclusions

We characterized the intermolecular complexes of a rare-gas molecule, HXeOH, with water. The data of the IR matrix-isolation studies and of ab initio quantum chemical calculations show that complexes of HXeOH with water molecules are actually formed. Their equilibrium configurations are consistent with the distributions of electron densities: a large positive charge on Xe in HXeOH prevents a straightforward grouping of water molecules around the anionic fragment OH^- of HXeOH, and the lowest energy structures of the complexes $HXeOH-(H_2O)_n$ correspond to the chains of water molecules spread along the O−Xe−H axis (see Figure 2). In addition, other structures with rather similar but somewhat higher energies may be formed. According to the results of quantum chemistry modeling, the computed shifts of the Xe−H stretching mode upon complexation of HXeOH with one and two water molecules are in good agreement with the experimental observations (peaks C_1 and C_2 vs the HXeOH monomer peak in Figure 1).

Similarly to the HXeOH monomer, the complexes of HXeOH with water molecules are metastable moieties, which can be decomposed upon some activation. Theoretical analysis of the decomposition routes of $HXeOH-(H_2O)_n$ ($n = 0, 1, 2, 3$) allows us to conclude that these reactions can proceed through either bent or linear transition states. In the first case (bent TS), the rare-gas species decompose to the true lowest energy products, $Xe + (H_2O)_{n+1}$, while in the linear TS, the Xe−H bond breaks, and the system relaxes to another local minimum. Due to decomposition via the bent TS, the number of water molecules attached to HXeOH can hardly exceed two. This is a result of the orientation of water molecules around the stable species HXeOH favoring the equilibrium geometry close to the bent TS. According to the calculations, the HXeOH monomer and its complexes with one and two water molecules are fairly stable in this respect, since the activation barriers are estimated at the MP2 level as 39.6, 26.6, and 11.2 kcal/mol, respectively.

Our simulations show that water molecules attached to the HXeOH monomer lead to some increase of the positive charge of the XeH fragment, which strengthens the H−Xe covalent bond and blue-shifts the corresponding stretching frequency. The surface-like structures, in which the "tail" Xe−H is fairly free of surrounding water molecules, were computationally predicted for the complexes $HXeOH-(H_2O)_n$. These structures may survive decomposition to $Xe + (H_2O)_{n+1}$ via the bent transition state. It is reasonable to assume that, in the mixed xenon−water clusters, the species HXeOH may also survive decomposition with the rupture of the Xe−H and O−Xe bonds.

Acknowledgment. The Academy of Finland supported part of this work. The Russian coauthors thank the Russian Foundation for Basic Research (Project 01-03-32071).

Supporting Information Available: Tables of Cartesian coordinates and total energies of the computed stationary points (PDF). This material is available free of charge via the Internet at http://pubs.acs.org.

JA0266870